

# A simulation framework for autonomous lunar construction work

Mattias Linde<sup>1</sup>, Daniel Lindmark<sup>1</sup>, Sandra Ålstig<sup>1</sup>, and Martin Servin<sup>\*1,2</sup>

<sup>1</sup>Algoryx Simulation AB, Umeå, Sweden

<sup>2</sup>Department of Physics, Umeå University, Umeå, Sweden

\*Corresponding author: martin.servin@umu.se

## Abstract

We present a simulation framework for lunar construction work involving multiple autonomous machines. The framework supports modelling of construction scenarios and autonomy solutions, execution of the scenarios in simulation, and analysis of work time and energy consumption throughout the construction project. The simulations are based on physics-based models for contacting multibody dynamics and deformable terrain, including vehicle-soil interaction forces and soil flow in real time. A behaviour tree manages the operational logic and error handling, which enables the representation of complex behaviours through a discrete set of simpler tasks in a modular hierarchical structure. High-level decision-making is separated from lower-level control algorithms, with the two connected via ROS2. Excavation movements are controlled through inverse kinematics and tracking controllers. The framework is tested and demonstrated on two different lunar construction scenarios that involve an excavator and dump truck with actively controlled articulated crawlers.

## Keywords

Lunar construction; Excavation; Physics-based simulation; Automation; Behaviour trees.

## 1 Introduction

Planning construction work on the Moon, such as the Artemis project lunar base, is a challenging task. Many aspects remain unknown, including local ground conditions, how the machines should be designed and operated to accomplish the task within the stipulated time and adhere to limited energy budgets. The machines should possess a high degree of autonomy due to the significant delays associated with remote control from Earth. Additionally, it is important that multiple machines can work in a well-coordinated manner, avoiding idle times and utilizing the equipment as efficiently as the energy supply allows for.

To succeed in this and similar tasks, simulation-based tools are crucial for studying how different configurations of the lunar conditions, machine design, and control system affect the time and energy consumption in a given construction project. These tools are also essential for detecting weaknesses in the entire approach and reducing the risk of severe failures. Additionally, such tools can also be used for generating large amounts of synthetic data for training deep learning models. To effectively iterate over numerous scenarios, each involving long sequences of machine operations, the simulations must be highly computationally efficient while remaining sufficiently realistic in terms of forces, power consumption, material flow, and vehicle behaviour. Furthermore, it must be easy to define and test different work plans, autonomous functions, and combinations of sensors.

To this end, we develop a framework for simulating autonomous ground construction tasks in a lunar environment. The framework leverages physics-based simulations of autonomously controlled construction machines interacting with dynamic terrain, utilizing the AGX Dynamics realtime physics engine [1, 17]. The systems' autonomous control is modeled using behaviour trees [7, 9], which enables the representation of complex behaviours (tasks) through a discrete set of simpler tasks organized in a hierarchical and modular structure. High-level decision making is performed in the behaviour tree, whereas low-level control algorithms are handled by skills on the different machines. This approach makes it easy to replace and introduce new capabilities and new machines. Communication between the machine's controller and the current state of the lunar environment occurs via ROS2, simplifying the replacement of virtual components with their physical counterparts.

Our main contribution in the present work is a description of said framework and results from testing it on two scenarios, namely extracting lunar regolith and excavating a predefined ground structure. The tests involve one excavator and one dump truck, but the framework is inherently designed to support many different machines. The work illustrates that the framework supports analysis of how the construction performance and energy use depend on different environmental factors.

### 1.1 Related work

There are few prior publications on simulation frameworks for autonomous lunar construction. A recent work is the framework introduced in [5]. It supports synthetic sensors, vehicle dynamics, and terramechanics using the Chrono physics engine. The terramechanics models include the Soil Contact Model (SCM) for wheel-terrain interaction, and continuum (SPH) and discrete (DEM) soil models for general use, including excavation and

bulldozing. The SynChrono module give support for multi-agent systems, e.g., sharing of state information with synchronised but distributed simulation across computing nodes. The simulations involving ground construction work are too computationally intense for use in applications with realtime or higher performance. Case studies in the paper focus on generation and analysis of synthetic images using physically-based rendering for realistically capturing lunar lighting conditions.

In [20], autonomous multirobot excavation for lunar applications was controlled using artificial neural tissue (ANT), trained using multi-agent grid world simulations and evaluated using a higher-fidelity 3D simulation based on the tool Digital Spaces with the fundamental earthmoving equation for bucket-soil interaction [8]. Modeling or analysis of power transmission and consumption is not addressed. In simulation, the ANT controller was found to achieve 30% better fitness (target grid cells being excavated) than with a conventional neural network.

From NASA, the Digital Lunar Exploration Sites Unreal Simulation Tool (DUST) [6] makes lunar terrain data and several computational tools available in the Unreal Engine 3D environment to support the Artemis mission. NASA-Ames and Open Robotics have developed a Gazebo-based lunar rover simulator. Wheel-terrain interaction is accounted for by empirical drawbar-pull and slip models, and terrain deformations are not supported.

OmniLRS is a simulation framework under development that uses IsaacSim from NVIDIA for photorealistic simulation of planetary rovers on lunar terrain [15] with a data-driven wheel-terrain interaction model [10]. As far as we are aware, the framework does not support excavation or bulldozing.

In [19], a tracked excavation rover platform was studied in simulations based on the Vortex physics engine from CM Labs and by field experiments. No conclusions were reported.

Teleoperation tasks for lunar surface construction, in particular excavation, were studied in virtual reality using the Unity Engine in [16] to examine the effect of time delay. The outcomes indicate that time delays significantly degrade task performance, and the operators modify their control strategies to cope with the time delay conditions.

None of the related work offers the combined functionality of realtime physics-based simulation of lunar construction work and representation of complex behaviour of autonomous machines for executing the construction work plan.

## 2 Method

This section introduces the underlying methods for physics-based simulation, behaviour tree-based task planning for multiple mobile machines, and ROS for interconnecting them.

### 2.1 Physics-based simulation

For modeling and simulation, we rely on the physics engine AGX Dynamics [1]. It is based on the framework for contacting multibody dynamics introduced in [12], extended to the discrete elements in [18], and to dynamic deformable terrain in [17]. Specifically, it uses maximal coordinate representation in terms of rigid bodies and kinematic constraints for joints, motors, and frictional contacts. This has been used in previous work to develop machine learning models for autonomous control of earthmoving equipment [3, 4] and active suspension system for rough terrain navigation [21] with successful transfer of controllers trained in simulation to reality of working [22].

The time-stepper and solver are optimized particularly for fixed timestep realtime simulation of multibody systems with non-ideal constraints and non-smooth dynamics [11]. The hybrid direct-iterative solver supports fast and stable simulations at high accuracy for mathematically stiff and ill-conditioned systems [11], such as robots and vehicles, and scalability to large-scale dynamic contact networks, such as for granular systems, at the price of lower accuracy [18].

For deformable terrain, AGX uses the multiscale model described in [17]. It has been demonstrated to produce digging forces and soil displacements with an accuracy of 75-90% of that of a resolved discrete element method (DEM), coupled with multibody dynamics, and with field tests involving full-scale construction equipment [2]. The model can be regarded both as a reduced-order model of DEM and as a multibody dynamics generalization of the FEE. The idea is to dynamically resolve only the part of the terrain inside a well-localized region of shear failure. The terrain is assigned a set of bulk mechanical parameters for its physical behaviour in nominal bank state. When a digging tool contacts the terrain surface, a zone of active soil displacement is predicted. Only inside the active zone is the soil resolved into particles. These are modeled using DEM with specific mass density and contact parameters that ensure a bulk mechanical behaviour consistent with the assigned bulk parameters through a pre-calibration procedure. See, Ref. [17] for details. The reaction force on the bucket consists of frictional-cohesive contacts with an aggregate body, which inherits the physical properties of the soil in the active zone, and a penetration resistance constraint, which is a function of the bucket geometry, soil parameters, and the soil pressure at the cutting edge.

The particle size varies dynamically in the multiscale model by mass exchange between particles and with the terrain. This provides a balanced tradeoff between fine resolution, close to the bucket cutting edge and the terrain surface, and coarser elsewhere. To avoid the DEM simulation being a computational bottleneck, large particles are favored by the algorithm. With the multiscale approach, the errors in digging forces remain smaller than if the terrain were composed of DEM particles. However, large particles misrepresent the real soil flow and distribution

inside the bucket. Specifically, the volume fraction is overestimated at the soil-bucket interface. Consequently, with large particles the bucket filling is typically underestimated unless one compensates by assigning the particles a higher mass density by a factor proportional to the particle cross-section area over the bucket's internal surface area.

The terrain model can also be assigned to dynamic bodies, such as the load-carrying truckbed of a dump truck. Terrain particles that are dumped and settling to rest, are converted to a local terrain that co-moves with the dump truckbed and adds to its mass and inertia tensor. When the truckbed is raised and tilted to a critical angle, the terrain starts avalanching and is resolved into particles until they come to rest again.

## 2.2 Behaviour trees

To achieve modular, scalable, and explainable machine behaviours, behaviour trees (BT) are utilized. They are widely used in artificial intelligence applications for representing task switching policies. See [9] and [7] for an in-depth treatment. A BT is a rooted tree structure where the nodes are connected with parent-child relationship. When the tree is *executed*, or *ticked*, traversal begins at the root and proceeds according to the types of nodes and the status of the nodes. Each node returns one of the following status values, *Success*, *Failure*, *Running* and the status values affect the traversal for the common node types in the following way:

**Sequence** A sequence node ticks all its children in order. If any child returns *Failure* or *Running*, the sequence halts and returns the same status. The sequence returns *Success* only if all children succeed.

**Selector** A selector node, also called fallback node, ticks its children in order until one returns *Running* or *Success* and the selector will return the same status. If all children fail, then the selector also returns *Failure*.

**Parallel** A parallel node ticks all children concurrently. A policy (e.g. succeed on one, succeed on all, succeed on specific child) determines how the children's statuses are aggregated into the parallel nodes return status.

**Decorator** A decorator is a node with a single child that can change the child status, e.g. an Inverter swaps *Success* and *Failure*.

**Condition** A condition is a leaf node that checks a condition and returns either *Success* or *Failure*.

**Task** A task or action is a leaf node that represents an action. It returns *Running* while the action is ongoing, *Success* when the action is completed, and *Failure* if the action could not be performed.

## 2.3 Robot Operating System

Robot Operating System (ROS) is a middleware framework for robot software development [14]. It provides tools, libraries, and conventions for creating complex and robust robot behaviour across different robotic platforms. With standardised interfaces, ROS encourages modular development with packages for specific robotic functionalities and services designed for heterogeneous computer clusters, including hardware abstraction and low-level device control. With ROS2, it also functions as a middleware for communication [13]. The message-passing interface enables independent processes, nodes, to communicate via publications and subscriptions.

## 3 Simulation framework

This section begins with a general overview of the autonomous construction framework, followed by a detailed explanation of how its components are used to control machines for performing autonomous tasks.

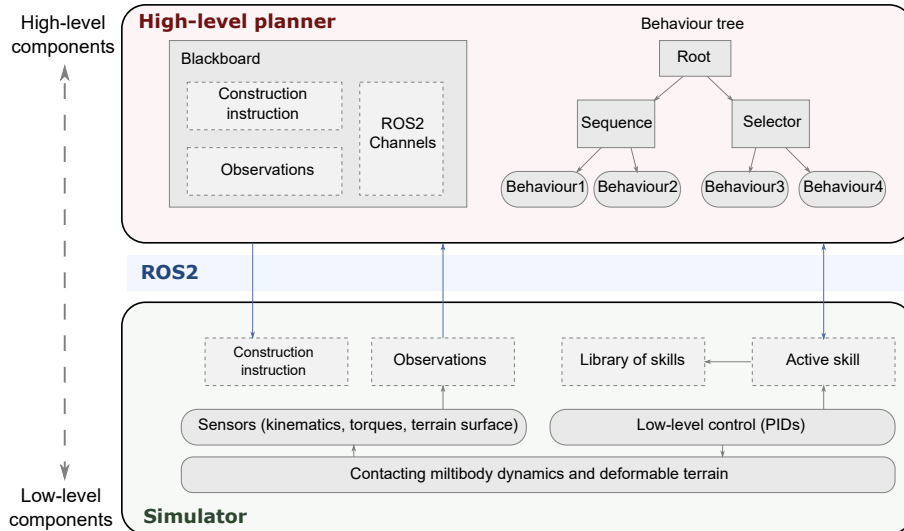


Figure 1: Overview of the framework with its two main components, the high-level planner and the simulator interconnected with ROS.

The autonomous simulation framework is implemented in Python and consists of two main components: *a high-level planner* and a *simulator*. These components run as separate processes and communicate using ROS2. This separation introduces a key feature: the planner does not have direct access to the ground truth of the world state, as that information resides within the simulator. Instead, the planner must rely on observations being sent from the machines to update its own world state. Although there is no technical barrier preventing the components from being in the same process, maintaining them as separate processes offers several advantages. It enhances modularity, facilitates the replacement of individual parts and supports the development of more robust autonomous systems where perfect information cannot be assumed. Furthermore, this architecture simplifies future extensions, such as introduction of extra communication delays or disturbances. An overview illustration of the framework is found in Fig. 1.

### 3.1 High-level planner

The tasks to be performed by the planner are defined using a behaviour tree. This tree is composed of PyTrees’ built-in *composites* and *decorators*, along with a set of predefined framework behaviours, and when necessary, user-defined behaviours. Tree nodes can share data via a common blackboard and may add information for future node ticks. The framework makes use of the *memory* feature for sequence nodes — where the status *running* results in the sequence being restarted from the running node on the next tick instead of from the beginning.

Users define the behaviour tree using a structured text format. Each non-empty line includes an *optional node name*, a *node specification* and an *optional machine context*. Indentation levels are used to indicate parent-child relationship between nodes. Comments can also be added using a simple annotation format. The node specification can either reference a class name or a Python method that returns a node or subtree. This allows for modular reuse of subtrees across different machines, minimizing code duplication. The machine context, specified as `-> machinename`, indicates which machine a subtree should interact with. This enables the reuse of identical node types multiple times within a tree, each instance operating on a different machine. An example of textual representation of a behaviour tree is illustrated in Fig. 2 with the corresponding tree representation in Fig. 3.

```

Root: Sequence
  Parallel: ParallelSuccessOnFirst
    # Scenario completed? -> Tree Success
    Scenario: Sequence
    ...
    # Decorator between machine subtrees
    # and parallel node are omitted.
    Machine1: Sequence -> excavator1
    ...
    Machine2: Sequence -> dumptruck1
    ...

```

Figure 2: Example of a textual representation of a behaviour tree. Dots are used to indicate omitted nodes or subtrees to keep the example short.

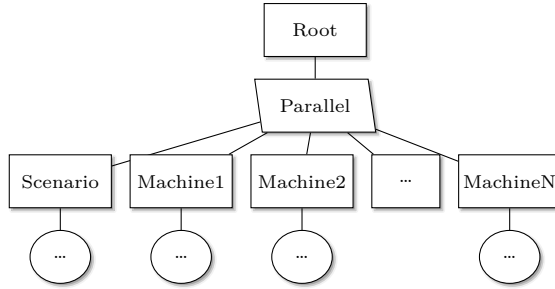


Figure 3: Example structure on a high level for a behaviour tree with multiple machines.

### 3.2 Simulator

The simulator component features a dynamic terrain and one or more machines. Each machine is equipped with a set of *skills* - capabilities that can be activated by the planner. Skills may also accept optional input data required for their execution. These skills correspond to specific actions that machines can perform through their low-level control systems.

Communication between the planner and simulator occurs over multiple ROS2 topics. Each node in the behaviour tree can have an associated skill on the machine, and the communication topic incorporates the machine context. For example, a topic could use `/[machine context]/target/drive` as name template. This naming convention allows generic nodes within the planners behaviour tree to interact with specific machines, supporting modular and scalable control logic. The same machine-context naming scheme is used for the planner to subscribe to telemetry and evaluation data from machines. These topics provide metrics such as execution time, energy consumption and skill status. Collecting this data enabled the assessment of a work plan’s efficiency and overall system performance.

**Case study:** *Excavating terrain to match a target profile.* To execute an excavation task using the autonomous framework, the process begins by selecting which machines will participate in the operation. Afterwards, a logical plan must be formulated outlining how the task should be executed, and then translated into a behaviour tree structure. With the tree setup, the next step involves preparing an initial configuration, currently done primarily using JSON files, which ensure that both the simulator and planner share a consistent initial view of the scenario configuration. Once this setup is complete, both components can be launched, allowing the machines to begin autonomous operation.

Assuming a similar structure as depicted in Fig. 3 and that a single excavator and one dump truck are involved, the behaviour tree structure offers a highly intuitive way to model and reason about the roles and actions of each machine. The use of a *parallel* node within the tree architecture allows each machine’s subtree to operate independently. This modularity simplifies the addition of new tasks or machines without devolving into the complexity associated with traditional state machines.

A logical breakdown of the excavator’s tasks is: if the bucket is empty, plan where digging should be performed and plan a drive trajectory towards the location, drive, and dig. If the bucket is non-empty, then a dig cycle has been completed, and then a dump cycle should be performed. If the bucket has material, plan where the material should be offloaded and plan a drive trajectory to the location, drive, wait for a dump truck to be in position, offload material. This workflow is illustrated in Fig. 4.

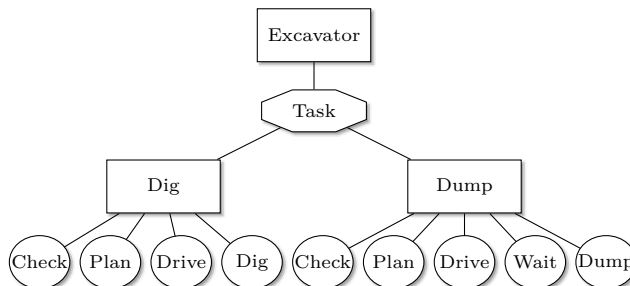


Figure 4: Subtree for an excavator.

The tasks for a dump truck can be divided and expressed in a similar way with two subtrees: Plan where to accept material and plan a route to the loading location if the truckbed is not full, then drive to the location. If the truckbed is full, plan where to offload material and plan a route to the target, wait until no excavator is offloading material, drive, and empty the truckbed.

The nodes shown in the subtrees in Fig. 4 and 5 map to functionality implemented in the framework. Nodes responsible for various types of planning do not activate machine skills directly. Instead, they carry out compu-

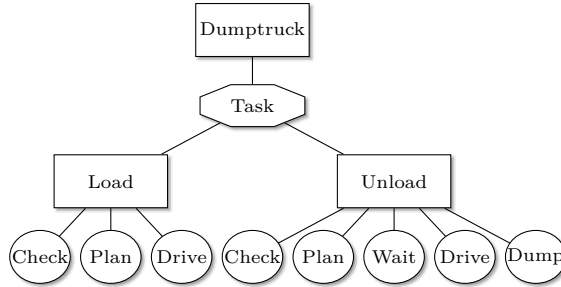


Figure 5: Subtree for a dump truck.

tation and store the result on the blackboard, allowing subsequent nodes to make use of that information. For instance, a drive node retrieves the precomputed route information, activates a driving skill on a machine, and passes along waypoint data required for execution.

To maintain execution integrity, especially in scenarios where certain tasks may fail and require re-execution, *FailureIsRunning* decorators are placed between a machine’s subtree and the parallel node. These decorators prevent PyTrees from reinitializing all subtrees in response to a failure, thereby supporting selective re-planning and robust recovery mechanisms.

The final portion of the behaviour tree addresses scenario completion. Determining when a scenario should be considered complete depends on how tasks, primarily the digging, are organized and carried out. A common strategy involves dividing the construction site into a local grid of cells, with the current cell index stored on the blackboard. During dig planning, the target profile is compared against the current world state for the active grid cell. If the current terrain matches the target within a predefined tolerance, the cell index is increased and planning restarted. If material needs to be removed, a dig trajectory is planned for the current active cell, taking the target profile into account. The scenario is considered complete when the final grid cell has been processed. This condition can be verified by a behaviour tree node that reads from the blackboard and checks if all grid cells have been successfully handled.

### 3.3 Motion planning and control

When the excavator should perform a certain task, for example digging out a section of the terrain, local joint-space values are needed that result in the end-effector performing the desired motion in task space. To compute these joint values, the Inverse Kinematics (IK) module in AGX Dynamics is used. The excavator model in the simulation contains all the information that is needed to do IK computations without specifying additional link lengths or joint positions. The attachment frames for the constraints already hold all the needed information, including possible joint ranges. Therefore, redesign of the machine can be done during prototyping without maintaining redundant values that risk becoming out of sync. The types of constraints that are supported are Hinge (rotational), Prismatic (sliding) and Lock (fixed).

The API for computing Inverse Kinematics in `agxModel` accepts an `AffineMatrix4x4` that contains the desired end-effector transform. That transform might not be reachable due to being e.g outside of the working range, or the desired orientation might not be achievable due to the degrees of freedom available in the mechanical structure.

To simplify the usage of IK computations, the `LunarExcavator` class has a method, `calculate_ik`, that accepts a world position and an angle versus the ground for the digging direction. This is to avoid requesting rotations in directions the excavator bucket can not physically rotate. Despite this, it is possible to request end-effector transforms which can not be realised by the machine.

When a transform can not be reached with sufficient precision, an error code is returned as well as the best joint values the IK-solver could find. These joint values can be used in a forward computation to see where the end-effector could go. Comparing the reachable transform with the requested transform is something a control algorithm can do as a step to decide how to proceed.

## 4 Numerical experiments

The framework was tested for its ability to support the analysis of autonomy solutions for lunar ground construction with multiple machines. This was done with numerical experiments covering two scenarios, one where lunar material is loaded and transported from an excavation area to a dump site, and a second one where the goal is to create a ground construction of a given shape. The simulations run approximately in realtime with a time-step of 10 ms with the behaviour tree accounting for about 0.3 ms of the computing time per time-step. Simulations were run on an AMD Ryzen 9 5900X desktop processor with 12 CPU cores and 3.7 GHz clock speed (GPU does not accelerate these simulations). Video material from the simulations can be found at <https://www.algoryx.se/papers/lunar-construction>.

#### 4.1 Construction machines and lunar environment

Both scenarios involve an excavator and a dumper. They are both equipped with crawlers with actively controlled sub-crawlers that promote high terrain mobility. When turning, the sub-crawlers are lifted to reduce turning resistance. While excavating and driving straight, the sub-crawlers are lowered to reduce sinkage and actively controlled to smoothly follow the terrain surface. The speed of the crawlers are controlled individually via a rotational motor for each sprocket. The motion of the sub-crawlers relative to the main crawler is also controlled via rotational motors.

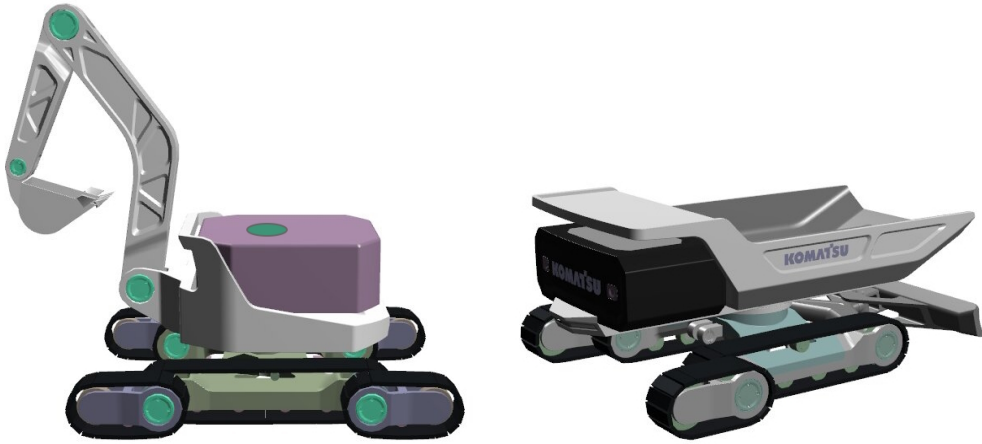


Figure 6: 3D models of the excavator and the dump truck. Actuated joints are marked in green. The machine width is 2.5 m.

The machines are 3.3 m long and 2.5 m wide. The excavator has 3 ton mass, and the empty dump truck weighs 2.0 tons. The actuators can deliver torque up to a maximum value but the required torques never reached these limits in the experiments. The target drive speed of the machines was 0.3 m/s when carrying a load and 0.35 m/s when driving empty. The crawlers were modelled using the AGX Tracks module. The number of track elements is about 50 and 20, for the main crawlers and sub-crawlers, respectively. To support numerical stability at integration with 10 ms time-steps, strong numerical viscous damping is enforced in the track element interconnection joints. That results in excessive power consumption when driving the crawlers. Therefore, the computed power was normalised by subtracting the dissipation observed when driving the tracks with no resistance from the terrain (having the vehicle elevated above ground) and introducing an efficiency factor (constant).

The lunar surface has an initial shape represented by an artificially generated elevation map. The terrain is given uniform soil properties, specifically the regolith was assigned a bank state internal friction angle of 0.80 rad, cohesion 900 Pa, dilatancy angle 0.23 rad, mass density of 1580 kg/m<sup>3</sup> at packing density 0.66, and compression index of 0.11. The local gravity acceleration is set to 1.6 m/s<sup>2</sup>.

Table 1: Mean and standard deviation for loaded and spilt mass, duration, and work over 30 cycles in Scenario 1 on flat and sloped terrain.

Case	Mass (kg)	Spill (kg)	Time (s)	Work (kJ)
Flat	$69 \pm 26$	$5 \pm 7$	$117 \pm 13$	$66 \pm 16$
Sloped	$64 \pm 24$	$4 \pm 5$	$118 \pm 15$	$74 \pm 24$

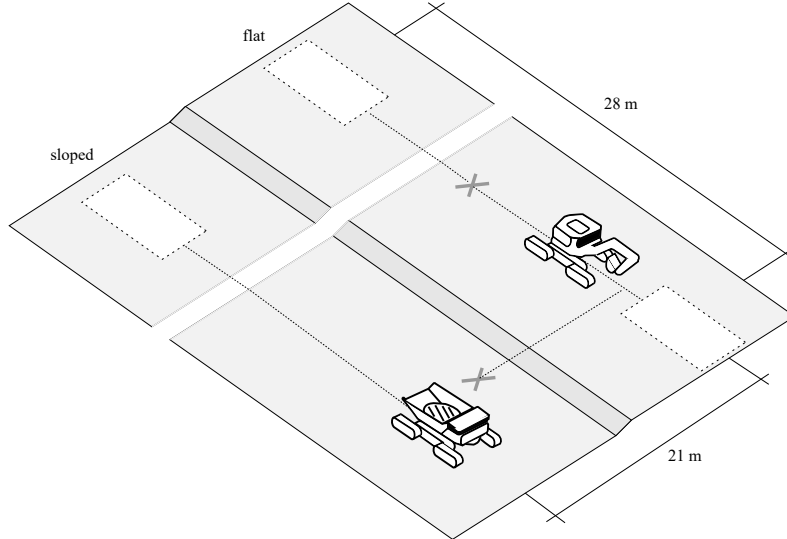


Figure 7: Illustration of Scenario 1 - Excavate lunar regolith from a dig area (right dashed rectangle), offloaded on a dump truck that carries the material to a dump area (left dashed rectangle) where it is offloaded. Two dump areas are considered, separated by a slope. The scales are not accurate to the real scene.

#### 4.2 Scenario 1 - Excavate, haul, and dump lunar regolith

The construction instruction in this scenario was to repeatedly excavate and move soil from a dig area to a dump area with boundaries specified by coordinates. The excavator and dump truck have behaviour trees as described in the previous section.

Two variations of the scenario were made, and we refer to them as *flat* and *sloped*. They differ by the location of the dump area. In the flat case, the dump area is located in the same region of rather flat terrain as the dig area. See Fig. 7 for an illustration. In the sloped case, the dig and dump areas are separated by a slope that the excavator must cross each digging cycle to reach the dump truck at the lower region. The distance to reach the dump truck from the dig area is, on the other hand, 20% shorter on average in the sloped case.

The dump truck will start the dumping process when its target load is reached. When driving to the dumping position, an extra waypoint will be created where the dump truck will get the correct dumping orientation. It will then drive straight to the final position. This is to avoid unwanted interaction between the pile and the dump truck. When dumping, the dump bed will rest in a raised position for a couple of seconds. The dump truck will then move forward with the bed still raised before lowering the bed and driving towards a loading position.

The construction work was simulated over 30 digging cycles, and virtual sensor data was collected, including time series for vehicle pose, kinematics, actuator torques, and loaded and dumped soil mass. Power consumption was computed by integrating the (positive) work exerted by the actuators. Image sequences from the two simulations can be found in Fig. 8.

A summary of the results is found in Table. 1. The average loaded mass was 8% higher in the flat case. This is attributed to the fact that it is more difficult to track the excavator's planned path across the slope than over the flat terrain. Consequently, the excavator sometimes ends up in a skewed pose where it is harder to fill the bucket. In both cases, there is material spilling (6-7%) from the bucket. This occurs mainly when turning the chassis, apparently causing too large peaks in acceleration. The average cycle times are very similar but the power consumption is 14% higher for the sloped case due to the slope traversal.

The evolution of the excavated and dumped mass, working time, and work per cycle are displayed in Fig. 9, 10, and 11, respectively. The moments when the excavator switches to a new cell are marked with dashed lines. We observe that the mass (and power consumption) drops at the switching events. This indicates that there is room for improving the planning to maximize the equipment utilization. The working time for different tasks is nearly constant, with the exception of when the excavator waits for the dump truck to return. The power consumption is dominated by running the crawlers although it was rescaled for the excessive dissipation mechanism for numerical stabilization. As can be more clearly seen in Fig. 12, the arm actuator dominates the power consumption during digging and varies a lot over the cycles, which can be understood by the fact that the planned bucket trajectory

adapts to the shape of the terrain, which evolves over time. We hypothesize that the greater power consumption in the sloped case is due to the fact that more uneven terrain leads to more situations where it is difficult, or even impossible, not to slip significantly with the large tracks.

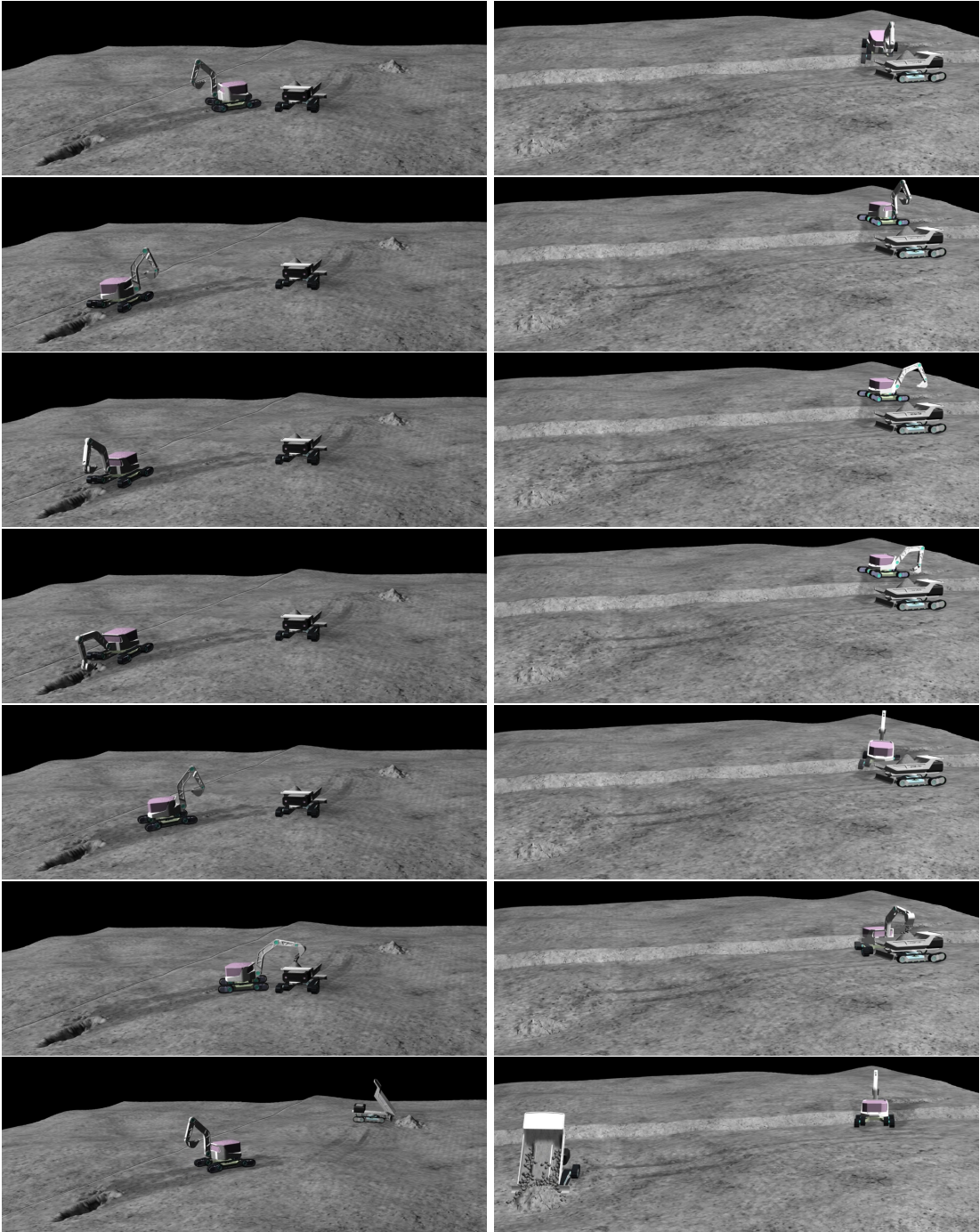
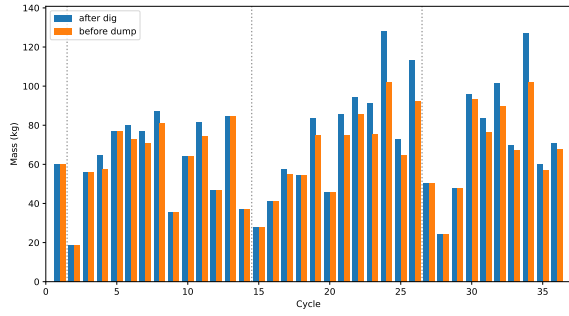
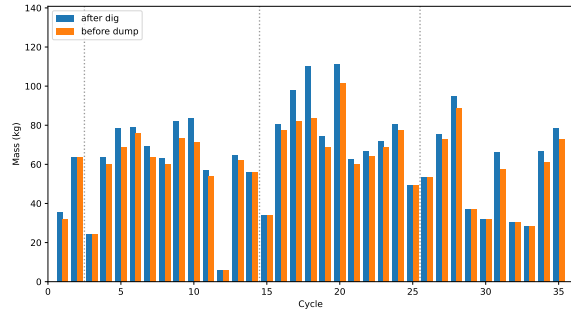


Figure 8: Image sequence from one excavation cycle in the scenario **Excavation-flat** (left) and **Excavation-slope** (right). The sequence ends with the crawler dumping its load at a dump area.

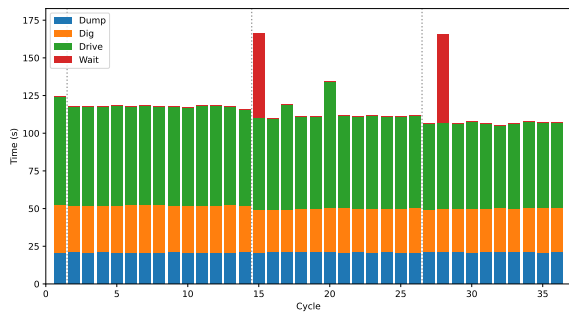


(a) flat

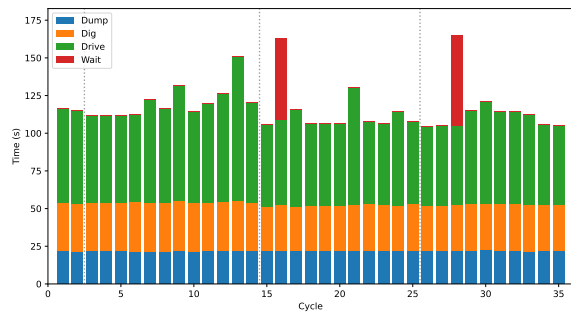


(b) sloped

Figure 9: Evolution of the excavated and dumped mass over 30 cycles for the two cases of Scenario 1.

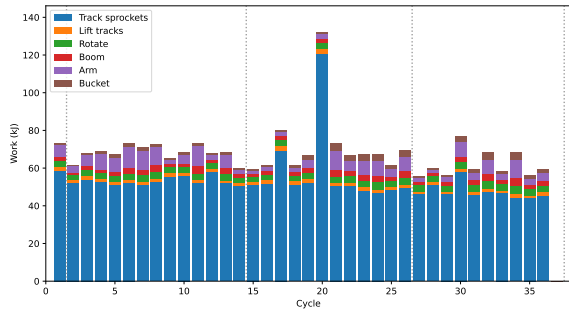


(a) flat

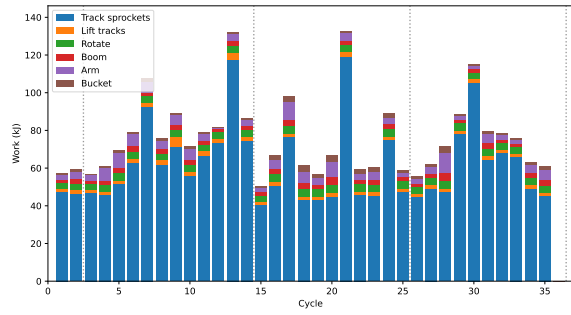


(b) sloped

Figure 10: Evolution of the working time over 30 cycles for the two cases of Scenario 1.



(a) flat



(b) sloped

Figure 11: Evolution of the work over 30 cycles for the two cases of Scenario 1.

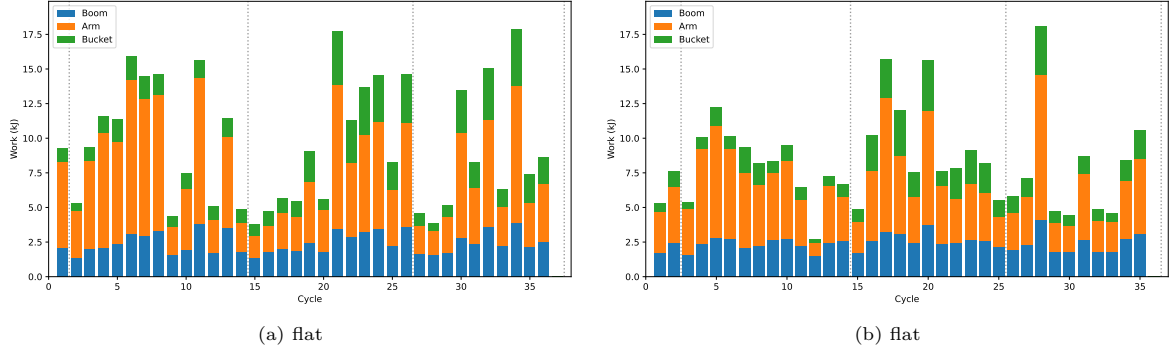


Figure 12: Evolution of the work for the excavation process only over 30 cycles for the two cases of Scenario 1.

### 4.3 Scenario 2 - Creating a predefined ground construction for habitat modules

In this scenario, an excavator and a dump truck collaborate to shape the terrain towards a specified 3D profile where habitat modules are to be placed and partially covered with regolith. The dump truck must adapt the location for parking to both the current dig location and the already excavated area in order to be easily accessible to the cycling excavator. See Fig. 13 for an illustration.

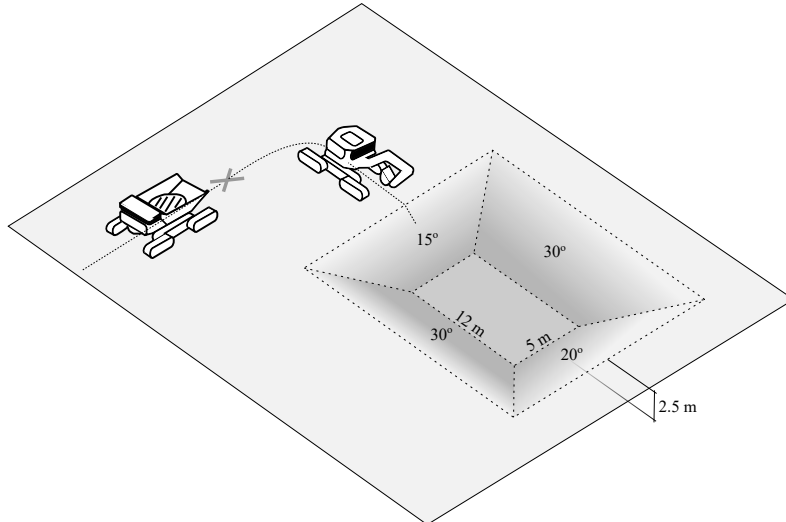


Figure 13: Illustration of Scenario 2 - Creating a predefined ground construction for habitat modules by repeated excavation and final grading using the dump truck blade.

The beginning of the scenario is displayed in Fig. 14 and the end in Fig. 15. When a cell is excavated, a new bucket tip trajectory is planned for each dig cycle. The positions are planned with the excavation depth down from the current terrain surface, but no deeper than the target surface or maximum digging depth. The target angle for the bucket is adapted to the target slope of the terrain. Excavating the entire structure would require roughly 10,000 work cycles which would amount to about a week of serial computing time. In our tests, we jumped to selected intermediate states and verified the operational performance over a sequence of cycles.

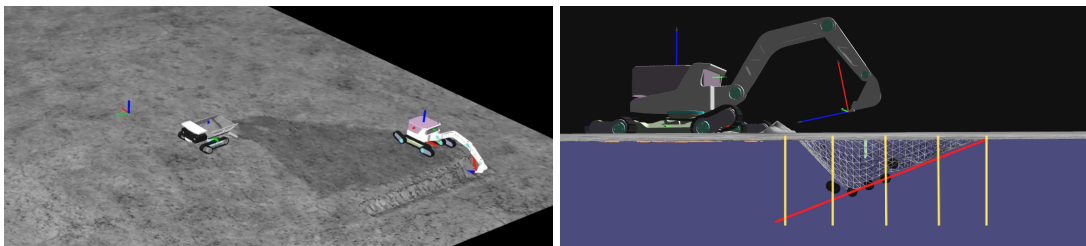


Figure 14: Beginning of excavating the ground construction for habitat modules. The lower image shows a cross-section with the target surface indicated in red and the estimated cell boundaries in yellow.

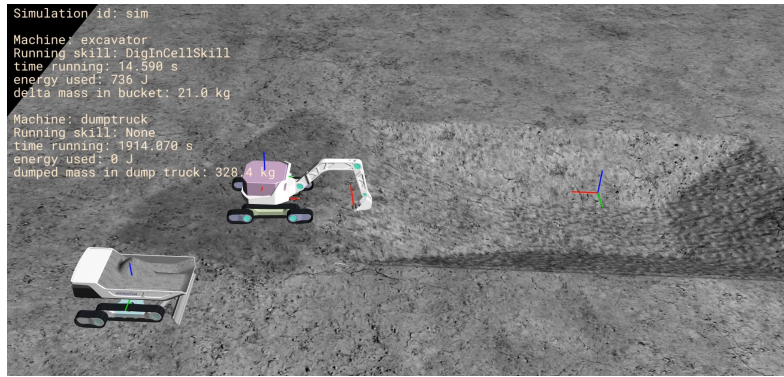


Figure 15: End of excavating the ground construction for habitat modules.

After the target 3D profile has been excavated, it is graded. When “grading” is used, the heights are different during the dig trajectory. If, on the other hand, the target profile is flat and “trench digging” is used, then a flat dig trajectory is used. For both cases, the shovel first reaches for a point slightly before and above the trajectory start, which improves the ability to get to the trajectory start with the specified angle.

During excavation, the terrain will avalanche, both sideways and also from the next row of cells that are closer to the excavator. Material from cells which have not been excavated yet will have material removed in the process of getting the current cell to its desired shape.

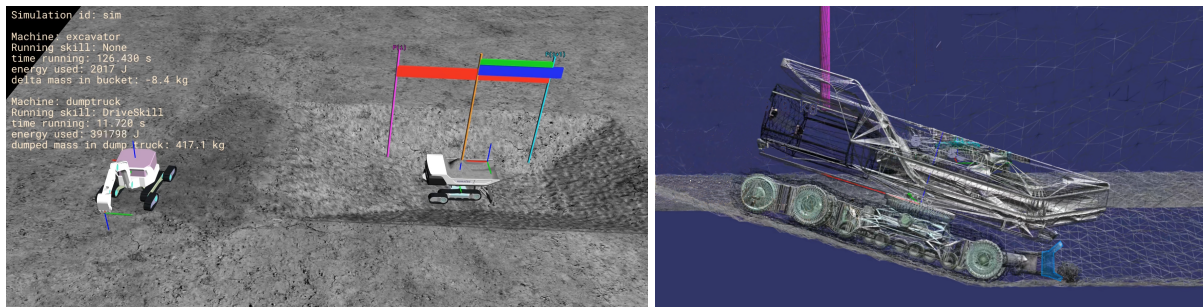


Figure 16: After excavating the ground construction for habitat modules, the excavator leaves room for the dump truck to perform final grading of the target surface. The lower image is a cross-section of the grading with the actively controlled blade highlighted in blue.

The dump truck operates as in the previous scenario until the excavator has finished grading the target shape. The dump truck is then performing final grading of the bottom of the shape using its blade, see Fig.16 The `leveling/start_position`, `leveling/end_position`, and `leveling/offset` variables from the last work setting provided are used to plan out a series of runs across the bottom of the shape. These runs are then performed with the shovel lowered to level the terrain. The blade position is dynamically adjusted using a PID controller with parameters provided by the machine manufacturer.

## 5 Conclusions

We have found that the simulation framework serves the purpose of analysing how a system for autonomous lunar construction performs under different circumstances, which can include differences in the lunar environment, machine design and control algorithms, and more. Future work should include more elaborate models for sensors and lunar soil, and explore the framework’s scalability for a large number of machines. The normalization procedure for compensating for numerical damping in the tracks should be experimentally validated to ensure that the energy computations are reliable. Automated generation and improvement of construction instructions using artificial intelligence is also interesting to evaluate.

## 6 Acknowledgements

The research was commissioned from Komatsu Ltd, which is commissioned for the Space construction innovation project as part of the Stardust Program in Japan, and supported in part by the Swedish National Space Agency through Rymdtillämpningsprogrammet dnr 2024-00310 (AILUR).

## References

- [1] Algorix Simulations. *AGX Dynamics*. Aug. 2025.
- [2] Koji Aoshima and Martin Servin. “Examining the simulation-to-reality gap of a wheel loader digging in deformable terrain”. In: *Multibody System Dynamics* (2024), pp. 1–28.
- [3] Koji Aoshima et al. “World Modeling for Autonomous Wheel Loaders”. In: *Automation* 5.3 (2024), pp. 259–281.
- [4] Sofi Backman et al. “Continuous control of an underground loader using deep reinforcement learning”. In: *Machines* 9.10 (2021), p. 216.
- [5] Nevindu M Batagoda et al. “A physics-based sensor simulation environment for lunar ground operations”. In: *arXiv preprint arXiv:2410.04371* (2024).
- [6] Lee Bingham et al. “Digital Lunar Exploration Sites Unreal Simulation Tool (DUST)”. In: *2023 IEEE Aerospace Conference*. 2023, pp. 1–12.
- [7] Michele Colledanchise and Petter Ögren. *Behavior Trees in Robotics and AI*. July 2018.
- [8] N Abu El Samid, Jekanthan Thangavelautham, and G D’Eleuterio. “Infrastructure robotics: A technology enabler for lunar in-situ resource utilization, Habitat construction and maintenance”. In: *Proceedings of International Astronautic Conference*. 2008, pp. 2045–2058.
- [9] Matteo Iovino et al. “A survey of Behavior Trees in robotics and AI”. In: *Robotics and Autonomous Systems* 154 (2022), p. 104096.
- [10] Junnosuke Kamohara et al. “Modeling of Terrain Deformation by a Grouser Wheel for Lunar Rover Simulation”. In: *arXiv preprint arXiv:2408.13468* (2024).
- [11] Claude Lacoursiere and Mattias Linde. “Spook: a variational time-stepping scheme for rigid multibody systems subject to dry frictional contacts”. In: *UMINF report* 11 (2011).
- [12] C. Lacoursière. “Ghosts and machines: regularized variational methods for interactive simulations of multibodies with dry frictional contacts”. PhD thesis. SE-901 87 Umeå: Umeå University, June 2007.
- [13] Steven Macenski et al. “Robot Operating System 2: Design, architecture, and uses in the wild”. In: *Science Robotics* 7.66 (2022), eabm6074.
- [14] Morgan Quigley et al. “ROS: an open-source Robot Operating System”. In: *ICRA workshop on open source software*. Vol. 3. 3.2. Kobe. 2009, p. 5.
- [15] Antoine Richard et al. “OmniLRS: A photorealistic simulator for lunar robotics”. In: *2024 IEEE International Conference on Robotics and Automation (ICRA)*. IEEE. 2024, pp. 16901–16907.
- [16] Miran Seo, Samraat Gupta, and Youngjib Ham. “Exploratory study on time-delayed excavator teleoperation in virtual lunar construction simulation: Task performance and operator behavior”. In: *Automation in Construction* 168 (2024), p. 105871.
- [17] Martin Servin, Tomas Berglund, and Samuel Nystedt. “A multiscale model of terrain dynamics for real-time earthmoving simulation”. In: *Advanced Modeling and Simulation in Engineering Sciences* 8.1 (2021), pp. 1–35.
- [18] Martin Servin et al. “Examining the smooth and nonsmooth discrete element approaches to granular matter”. In: *International Journal for Numerical Methods in Engineering* 97.12 (2014), pp. 878–902.
- [19] Masataku Sutoh. “Development and Evaluation of Mobility and Excavation Rover Toward Lunar Base Construction”. In: *Journal of Robotics and Mechatronics* 36.2 (2024), pp. 334–342.
- [20] Jekanthan Thangavelautham et al. “Autonomous multirobot excavation for lunar applications”. In: *Robotica* 35.12 (2017), pp. 2330–2362.
- [21] Viktor Wiberg et al. “Control of rough terrain vehicles using deep reinforcement learning”. In: *IEEE robotics and automation letters* 7.1 (2021), pp. 390–397.
- [22] Viktor Wiberg et al. “Sim-to-real transfer of active suspension control using deep reinforcement learning”. In: *Robotics and Autonomous Systems* 179 (2024), p. 104731.